Bilateral Thalamic Lesions

Alice B. Smith[1,2]
James G. Smirniotopoulos[1,2]
Elisabeth J. Rushing[1,3]
Steven J. Goldstein[4]

[1]Department of Radiology and Radiological Sciences, Uniformed Services University, 4301 Jones Bridge Rd., Bethesda MD 20814. Address correspondence to A. B. Smith (alsmith@usuhs.mil).

[2]Department of Radiologic Pathology, Armed Forces Institute of Pathology, Washington, DC.

[3]Department of Neuropathology and Ophthalmic Pathology, Armed Forces Institute of Pathology, Washington, DC.

[4]Department of Radiology, University of Kentucky College of Medicine, Lexington, KY.

OBJECTIVE. The purpose of this study was to present the neuroimaging findings and differential diagnosis of bilateral thalamic lesions.

CONCLUSION. The limited differential diagnosis of bilateral thalamic lesions can be further narrowed with knowledge of the specific imaging characteristics of the lesions in combination with the patient history.

Bilateral thalamic lesions are uncommon. These paired lesions have a limited differential diagnosis that includes metabolic and toxic processes, infection, vascular lesions, and neoplasia. The differential diagnosis can be further narrowed with the patient history, imaging characteristics, and presence or absence of lesions outside the thalami.

Primary Neoplasm

Bilateral thalamic glioma is a rare neoplasm, usually a diffuse low-grade astrocytoma (World Health Organization grade II), that occurs in both children and adults [1]. Bilateral thalamic glioma has a poor prognosis due to the location of the lesions [2]. Children typically have signs of increased intracranial pressure and movement disorders. Adults experience mental deterioration [1]. Typically, expansion of both thalami is accompanied by abnormal hyperintensity on T2-weighted images and hypointensity on T1-weighted images that is not associated with contrast enhancement. Hydrocephalus depends on the degree of mass effect. Diffusion is normal (Fig. 1).

Metabolic and Toxic Disorders

Many metabolic and toxic processes affect both thalami simultaneously.

Wernicke Encephalopathy

Wernicke encephalopathy results from a deficiency of vitamin B_1 and is frequently associated with alcohol abuse [3]. The classic clinical triad is ataxia, altered consciousness, and abnormal eye movements; however, the presentation is variable. Wernicke encephalopathy is a medical emergency managed with IV thiamine. T2-weighted MR images may show symmetric high signal intensity in the mamillary bodies, medial aspects of the thalami, tectal plate, periaqueductal gray matter, and dorsal medulla [4]. Contrast enhancement is variable. Thiamine is an osmotic gradient regulator, and deficiency can disrupt the blood–brain barrier, resulting in contrast enhancement [5]. Wernicke encephalopathy can have reduced diffusion (Fig. 2) owing to ischemia-like changes in the thalami that should be differentiated from true venous and arterial infarction [6].

Osmotic Myelinolysis

Osmotic myelinolysis accompanies rapid shifts in serum osmolality; the classic setting is the rapid correction of hyponatremia [7]. The classic lesion involves the central pons (central pontine myelinolysis). Other lesions affect the basal ganglia, thalami, and white matter (extrapontine myelinolysis). Acute T2 hyperintensity and T1 hypointensity occur in the affected regions. Contrast enhancement is uncommon, and reduced diffusion may be seen [8] (Fig. 3).

Fabry Disease

Fabry disease is an X-linked disorder of glycosphingolipid metabolism leading to accumulation of glycosphingolipids in the vascular endothelium, perithelium, smooth-muscle cells, heart, and brain that results in myocardial ischemia and stroke [9]. On T2-weighted images, lesions of high signal intensity due to the vasculopathy may be seen

in the deep white and gray matter. T1 hyperintensity in the pulvinar is a common and sensitive finding [10]. Pulvinar hypointensity may be seen on T2-weighted images but not consistently (Fig. 4). The cause of these changes in signal intensity is undetermined [9].

Fahr Disease

Fahr disease is a rare disease of unknown causation. It is characterized clinically by neuropsychiatric abnormalities and parkinsonian or choreoathetotic movement disorder. Extensive bilateral calcification of the deep gray matter is present and most frequently involves the globus pallidus (Fig. 5). Other areas of involvement include the putamen, caudate nuclei, thalami, and dentate nuclei [11]. Calcium–phosphorus metabolism is normal in these patients [11]. The T1 and T2 signal intensity in the calcified regions varies with disease stage and calcification [11]. The differential diagnosis of these parenchymal calcifications includes endocrinologic disorders such as hyperparathyroidism, hypoparathyroidism, and pseudohypoparathyroidism.

Wilson Disease

Wilson disease is an autosomal recessive inborn error of copper metabolism. Patients have cirrhosis, corneal Kayser-Fleischer rings, and degeneration of the basal ganglia. If the patient is not treated, the disease is progressive and fatal. MR images show symmetric T2 hyperintensity of the deep gray matter: putamina, globus pallidi, caudate nuclei, and the thalami. T1 signal intensity in the basal ganglia and thalami is usually reduced, but T1 signal intensity may increase owing to the paramagnetic effects of copper [12]. Contrast enhancement does not occur (Fig. 6). Evidence of restricted diffusion may be seen on early images and is followed by return to normal diffusivity after necrosis and spongiform degeneration have occurred [13].

Leigh Disease

Leigh disease is a genetically heterogeneous mitochondrial disorder in which progressive neurodegeneration leads to respiratory failure and death in childhood. Patients have elevated levels of lactate in the CSF, serum, and urine. On T2-weighted images hyperintensity may be seen in the involved regions, most frequently the basal ganglia, diencephalon, brainstem, thalami, and dentate nuclei [14]. MR spectroscopy reveals a decreased level of *N*-acetyl aspartate with elevated choline and lactate levels [15]. Contrast enhancement is uncommon (Fig. 7). In the acute phase, reduced diffusion may be seen.

Infection

Many viral forms of encephalitis involve the thalami, including West Nile encephalitis, Japanese encephalitis, Murray Valley encephalitis, Eastern equine encephalitis, and rabies. West Nile encephalitis is a single-strand RNA virus of the flavivirus family transmitted to humans from birds by culicine mosquitoes. It has been a summer seasonal epidemic in the United States since 1999.

West Nile encephalitis causes bilateral T2 hyperintensity in both thalami, the basal ganglia, and the midbrain. Sulcal T2 hyperintensity has also been reported, suggesting leptomeningeal inflammation [16] (Fig. 8). Contrast enhancement is variable. Reduced diffusion has been reported, most often in the posterior limb of the internal capsule, corona radiata, and subcortical white matter [16].

Creutzfeldt-Jakob disease (CJD) is a rare neurodegenerative disease caused by the accumulation of prion proteins in neurons. Persons with CJD experience rapidly progressive dementia. The disease is classified into three types. Most common ($\approx$ 85% of cases) is the sporadic form, of which no cause has been identified. The familial form accounts for approximately 15% of cases, and the infectious (variant CJD) or iatrogenic form is least common, making up less than 1% of cases. Imaging may reveal T2 prolongation and reduced diffusion in the basal ganglia, thalami, and cortex (cortical ribboning) [17] (Fig. 9). There is no contrast enhancement. Diffuse cortical atrophy occurs late in the course.

A key imaging finding in variant CJD is the pulvinar sign—high T2 signal intensity in the pulvinar (Fig. 10). This sign has a sensitivity of 68–90% for variant CJD and was once considered pathognomonic of variant CJD; however, it can also occur in sporadic CJD [18, 19]. The hockey stick sign (symmetric pulvinar and dorsomedial hyperintensity) is characteristic of variant CJD [18]. Cortical ribbon hyperintensity is rarely seen in variant CJD (Fig. 11).

Vascular Occlusion

Bilateral thalamic arterial infarcts are uncommon. The thalami are supplied by both anterior (anteroinferior thalami) and posterior (medial thalami) circulation, but several variations occur. Top of the basilar syndrome results in infarcts of the superior cerebellar and posterior cerebral artery territories (Fig. 12). The artery of Percheron, a variant, is a solitary arterial trunk arising from the proximal segment of the posterior cerebral artery and supplying the paramedian thalami and rostral midbrain bilaterally. Occlusion causes bilateral thalamic infarction.

Deep venous thrombosis typically results in bilateral symmetric involvement of the thalami and occasionally the basal ganglia. The causes include pregnancy, oral contraceptives, infection, trauma, and dehydration, but the cause is undetermined in 20–25% of patients [20]. An abnormally hyperdense vein may be seen on CT scans, and corresponding T1 hyperintensity from clot in the sinuses may be seen on MR images. CT and MR venography show no areas of contrast enhancement or signal intensity in the deep venous sinuses. Diffusion-weighted imaging may show heterogeneous signal intensity [21]. Patchy contrast enhancement may be seen (Fig. 13).

Mild to moderate cerebral hypotension causes reflex shunting of blood from the anterior to the posterior circulation to preserve the brainstem, basal ganglia, and cerebellum. Severe reduction in blood flow exceeds this mechanism, and protective shunting of blood no longer occurs. The result is damage to the deep cerebral nuclei, brainstem, and most active regions of the cerebral cortex [22]. Diffusion-weighted MRI is the earliest imaging technique to have abnormal findings [22] (Fig. 14).

Posterior reversible encephalopathy syndrome (Fig. 15) is a disorder of cerebral vascular autoregulation. The multiple causes, which are often but not always associated with hypertension [23], include glomerulonephritis, preeclampsia and eclampsia, and drug toxicity (cyclosporin). Symptoms include headache, seizures, and visual disturbance. CT and MRI typically show symmetric areas of vasogenic edema predominantly involving the posterior circulation. Localized mass effect, hemorrhage, and subtle enhancement are uncommon. Diffusion-weighted MRI findings usually are normal, but occasionally reduced diffusion occurs, suggesting the presence of cytotoxic edema [24].

Conclusion

Bilateral thalamic lesions have a variety of causes, and knowledge of the associated imaging findings can help narrow the differential diagnosis.

References

1. Partlow GD, del Carpio-O'Donovan R, Melanson D, Peters TM. Bilateral thalamic glioma: review of eight cases with personality change and mental deterioration. *Am J Neuroradiol* 1992; 13:1225–1230

2. Di Rocco C, Iannelli A. Bilateral thalamic tumors in children. *Childs Nerv Syst* 2002; 18:440–444

3. Ogershok PR, Rahman A, Nestor S, Brick J. Wernicke encephalopathy in nonalcoholic patients. *Am J Med Sci* 2002; 323:107–111

4. Zuccoli G, Gallucci M, Capellades J, et al. Wernicke encephalopathy: MR findings at clinical presentation in twenty-six alcoholic and nonalcoholic patients. *Am J Neuroradiol* 2007; 28:1328–1331

5. Doherty MJ, Watson NF, Uchino K, Hallam DK, Cramer SC. Diffusion abnormalities in patients with Wernicke encephalopathy. *Neurology* 2002; 58:655–657

6. Antunez E, Estruch R, Cardenal C, Nicolas JM, Fernandez-Sola J, Urbano-Marquez A. Usefulness of CT and MR imaging in the diagnosis of acute Wernicke's encephalopathy. *AJR* 1998; 171:1131–1137

7. Laureno R, Karp BI. Myelinolysis after correction of hyponatremia. *Ann Intern Med* 1997; 126:57–62

8. Cramer SC, Stegbauer KC, Schneider A, Mukai J, Maravilla KR. Decreased diffusion in central pontine myelinolysis. *Am J Neuroradiol* 2001; 22:1476–1479

9. Takanashi J, Barkovich AJ, Dillon WP, Sherr EH, Hart KA, Packman S. T1 hyperintensity in the pulvinar: key imaging feature for diagnosis of Fabry disease. *Am J Neuroradiol* 2003; 24:916–921

10. Moore DF, Ye F, Schiffmann R, Butman JA. Increased signal intensity in the pulvinar on T1-weighted images: a pathognomonic MR imaging sign of Fabry disease. *Am J Neuroradiol* 2003; 24:1096–1101

11. Avrahami E, Cohn DF, Feibel M, Tadmor R. MRI demonstration and CT correlation of the brain in patients with idiopathic intracerebral calcification. *J Neurol* 1994; 241:381–384

12. King AD, Walshe JM, Kendall BE, et al. Cranial MR imaging in Wilson's's disease. *AJR* 1996; 167: 1579–1584

13. Sener RN. Diffusion MR. imaging changes associated with Wilson's disease. *Am J Neuroradiol* 2003; 24:965–967

14. Valanne L, Ketonen L, Majander A, Suomalainen A, Pihko H. Neuroradiologic findings in children with mitochondrial disorders. *Am J Neuroradiol* 1998; 19:369–377

15. Sijens PE, Smit GP, Rödiger LA, et al. MR spectroscopy of the brain in Leigh syndrome. *Brain Dev* 2008; 30:579–583

16. Petropoulou KA, Gordon SM, Prayson RA, Ruggierri PM. West Nile virus meningoencephalitis: MR imaging findings. *Am J Neuroradiol* 2005; 26:1986–1995

17. Young GS, Geschwind MD, Fischbein NJ, et al. Diffusion-weighted and fluid-attenuated inversion recovery imaging in Creutzfeldt-Jakob disease: high sensitivity and specificity for diagnosis. *Am J Neuroradiol* 2005; 26:1551–1562

18. Collie DA, Summers DM, Sellar RJ, et al. Diagnosing variant Creutzfeldt-Jakob disease with the pulvinar sign: MR imaging findings in 86 neuropathologically confirmed cases. *Am J Neuroradiol* 2003; 24:1560–1569

19. Tschampa HJ, Mürtz P, Flacke S, Paus S, Schild HH, Urbach H. Thalamic involvement in sporadic Creutzfeldt-Jakob disease: a diffusion-weighted MR imaging study. *Am J Neuroradiol* 2003; 24: 908–915

20. Masuhr F, Mehraein S, Einhaupl K. Cerebral venous and sinus thrombosis. *J Neurol* 2004; 251: 11–23

21. Yoshikawa T, Abe O, Tsuchiya K, et al. Diffusion-weighted magnetic resonance imaging of dural sinus thrombosis. *Neuroradiology* 2002; 44:481–488

22. Huang BY, Castillo M. Hypoxic-ischemic brain injury: imaging findings from birth to adulthood. *RadioGraphics* 2008; 28:417–439

23. Ay H, Buonanno FS, Schaefer PW, et al. Posterior leukoencephalopathy without severe hypertension: utility of diffusion-weighted MRI. *Neurology* 1998; 51:1369–1376

24. Bartynski WS, Boardman JF. Distinct imaging patterns and lesion distribution in posterior reversible encephalopathy syndrome. *Am J Neuroradiol* 2007; 28:1320–1327
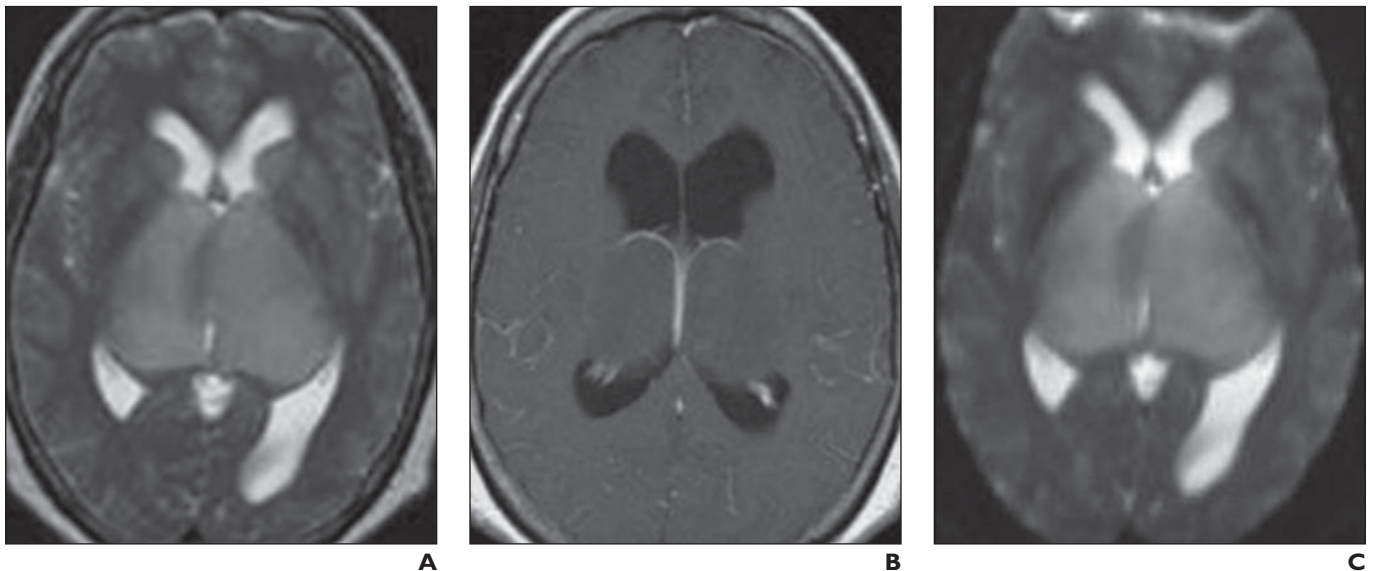
Fig. 1—52-year-old woman with bilateral thalamic glioma.
A, Axial T2-weighted MR image shows hyperintensity and bilateral diffuse enlargement of thalami resulting in hydrocephalus due to mass effect.
B, Axial T1-weighted gadolinium-enhanced MR image shows bilateral low signal intensity within thalami and no associated contrast enhancement.
C, Apparent diffusion coefficient map shows high signal intensity in both thalami.
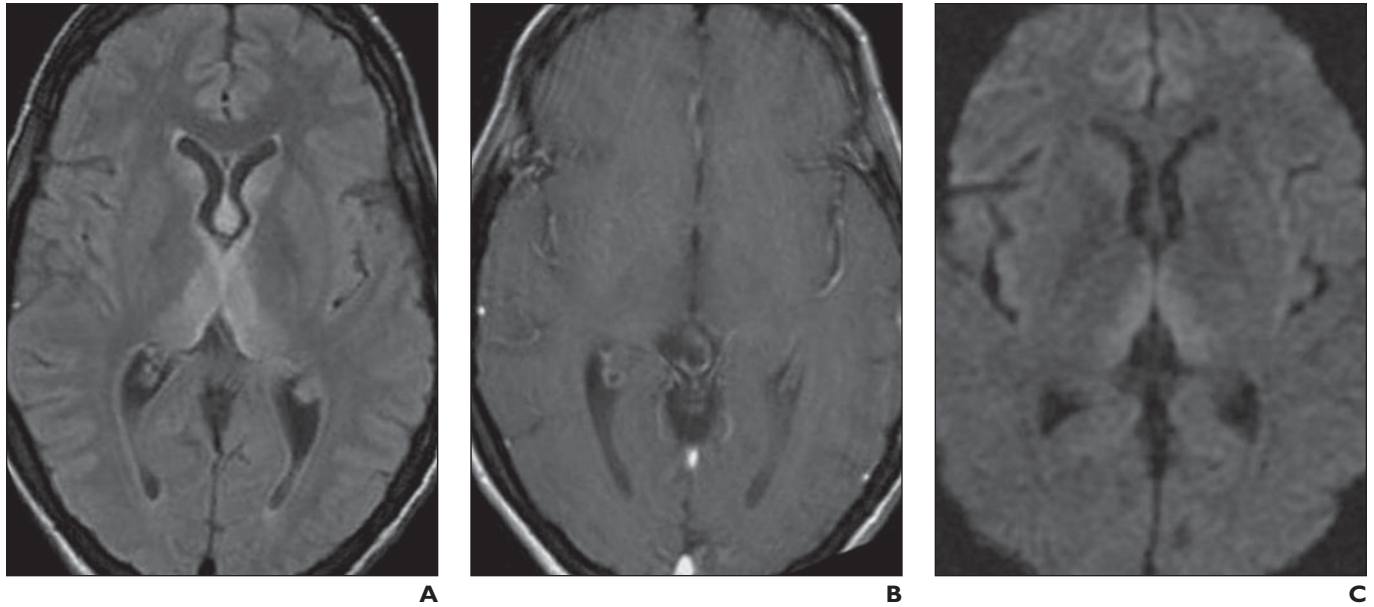
Fig. 2—52-year-old woman with Wernicke encephalopathy.
A, Axial T2-weighted FLAIR MR image shows hyperintensity in both thalami and to lesser degree in heads of both caudate nuclei.
B, Axial gadolinium-enhanced T1-weighted MR image shows no enhancement of thalami.
C, Diffusion-weighted MR image shows hyperintensity in both thalami consistent with reduced diffusion.
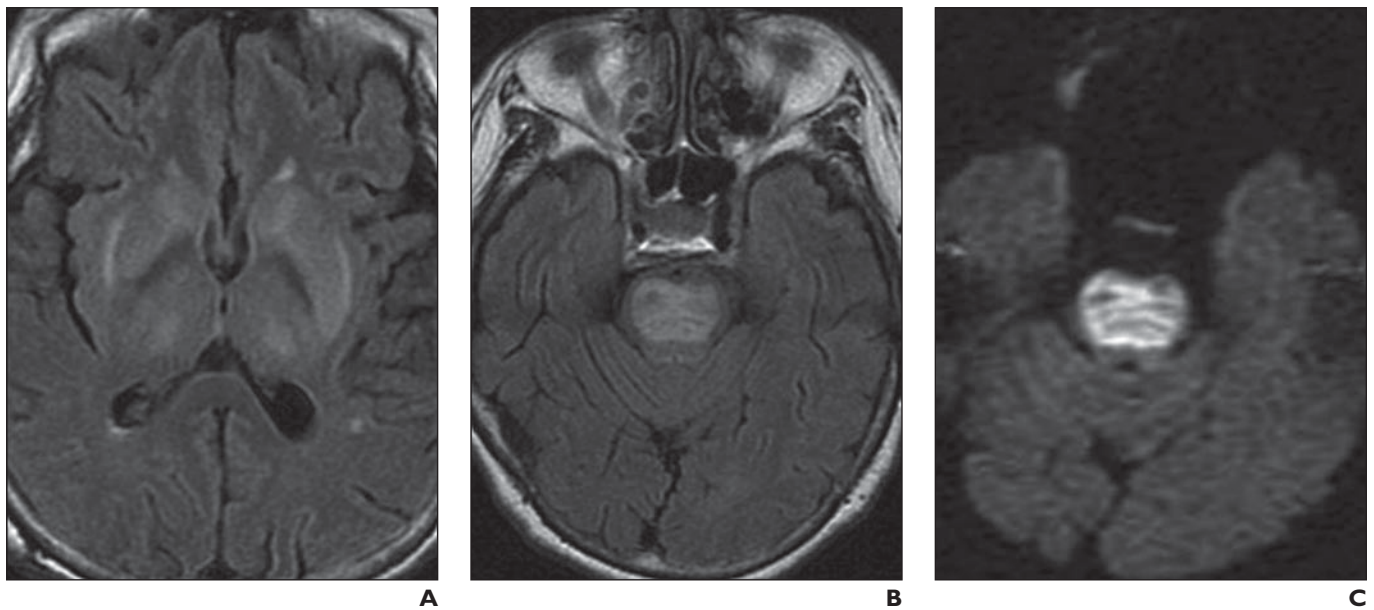
Fig. 3—28-year-old woman with osmotic myelinolysis.
A, Axial T2-weighted FLAIR MR image at level of basal ganglia shows hyperintensity involving basal ganglia and lateral aspects of both thalami.
B, Axial T2-weighted FLAIR MR image through level of pons shows symmetric hyperintensity involving central area of pons.
C, Diffusion-weighted MR image shows hyperintensity consistent with reduced diffusion involving pontine lesion.
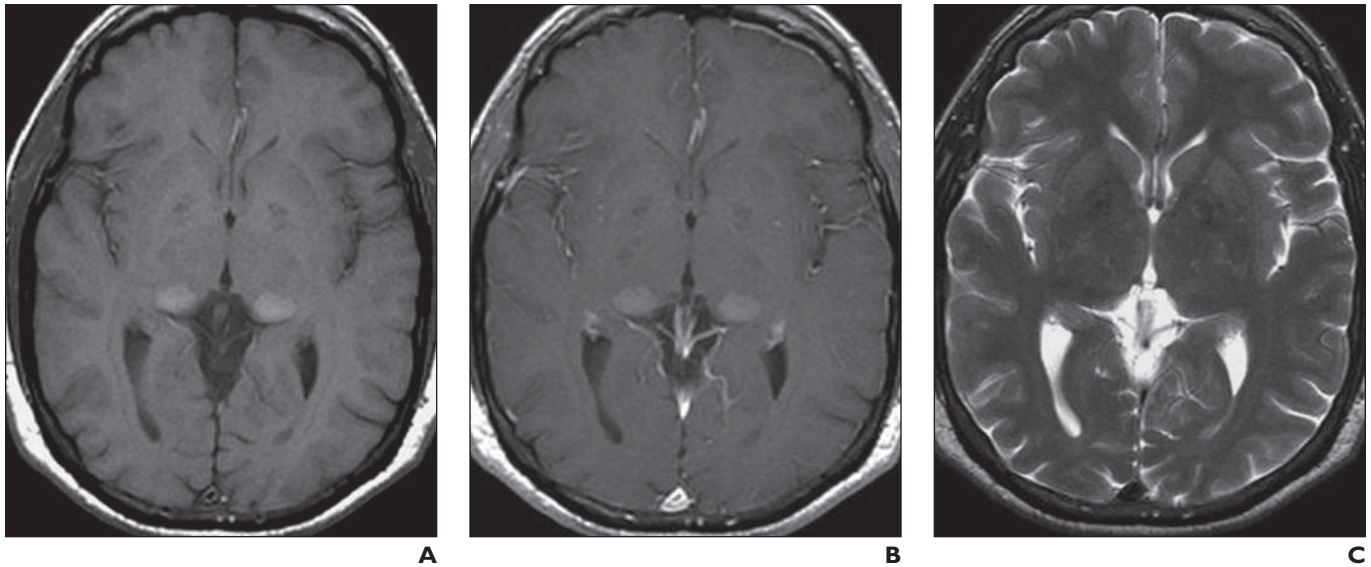
Fig. 4—47-year-old man with Fabry disease.
A, Axial T1-weighted MR image shows T1 hyperintensity involving both pulvinars.
B, Axial gadolinium-enhanced T1-weighted MR image shows no enhancement.
C, Axial T2-weighted MR image shows loss of signal intensity in both pulvinars.
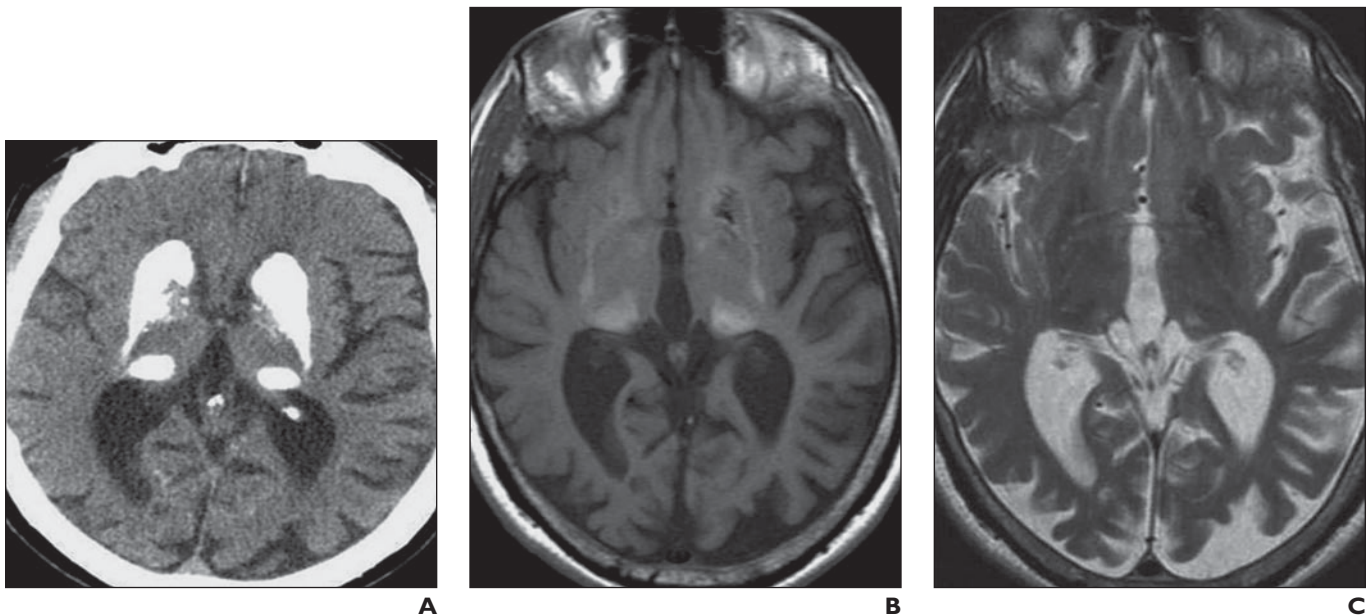
Fig. 5—45-year-old man with Fahr disease.
A, Axial unenhanced CT scan shows dense bilateral calcification involving basal ganglia and thalami. Within thalami, pulvinar are predominantly involved. Prominence of sulci and ventricles is greater than expected for age and is consistent with diffuse global volume loss.
B, Axial T1-weighted MR image shows high signal intensity in both thalami and heterogeneous signal intensity in basal ganglia.
C, Axial T2-weighted MR image shows predominantly low but heterogeneous signal intensity in basal ganglia and thalami.
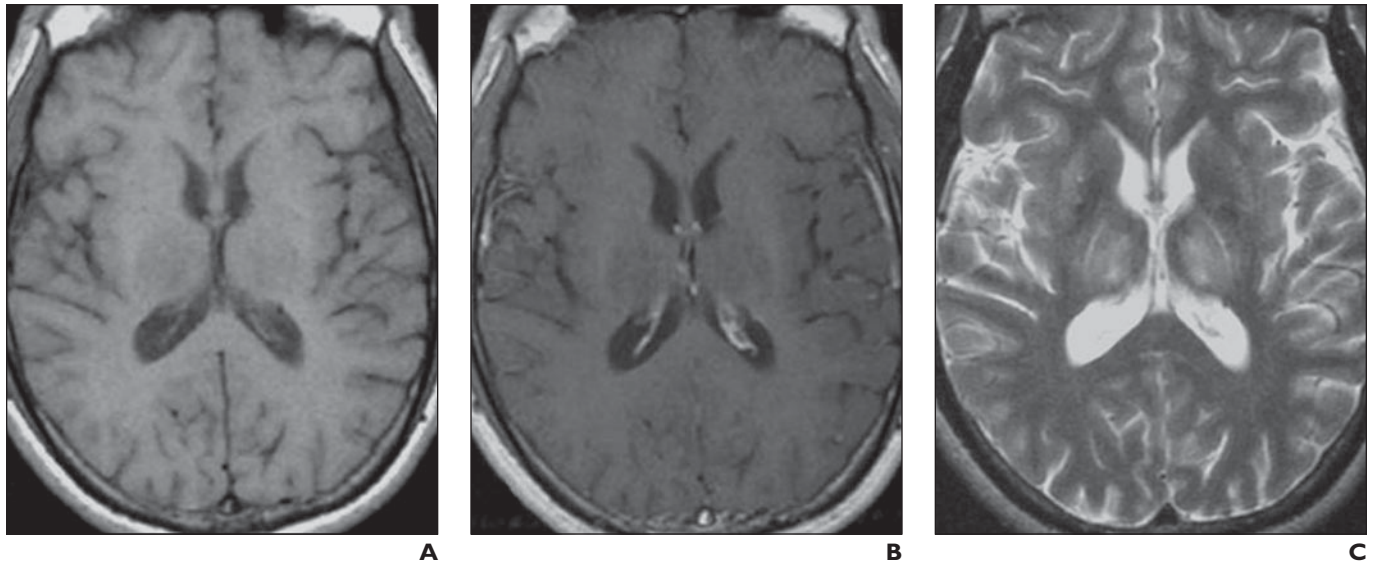
Fig. 6—18-year-old man with Wilson disease.
A, Axial T1-weighted MR image shows hypointensity of both thalami.
B, Gadolinium-enhanced T1-weighted MR image shows no enhancement.
C, T2-weighted MR image shows hyperintensity in both thalami and to lesser degree in both putamina.
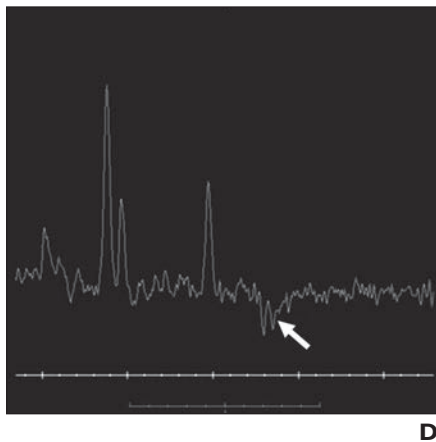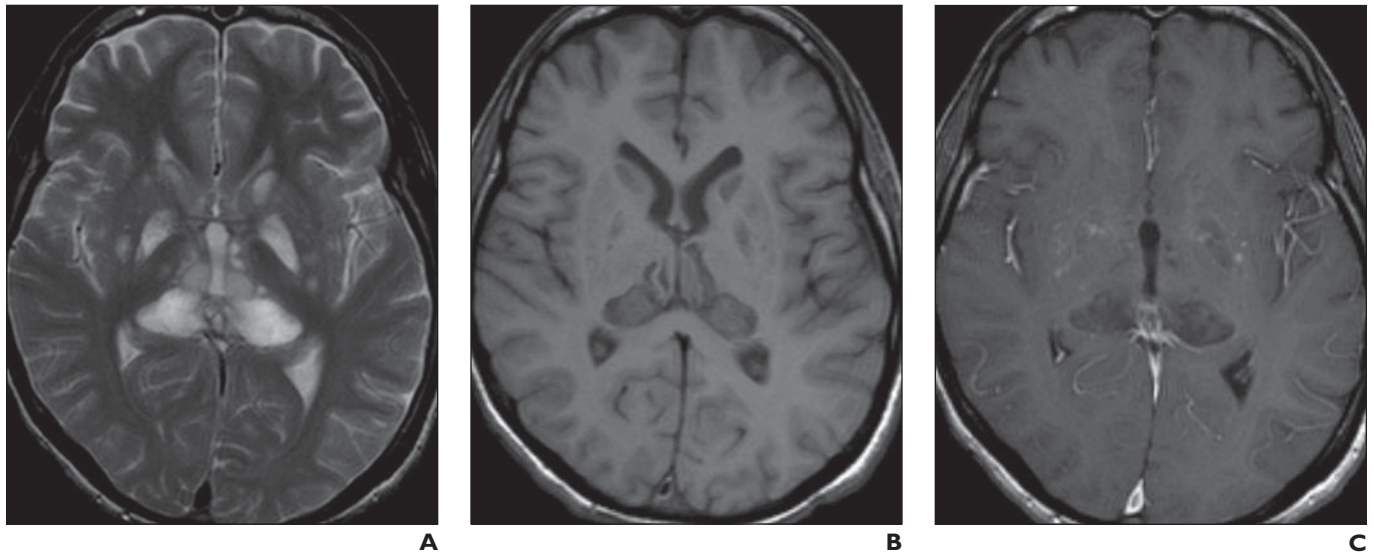
Fig. 7—16-year-old boy with Leigh disease.
A, Axial T2-weighted MR image shows bilateral area of high signal intensity involving thalami, globus pallidi, and to lesser degree, caudate nuclei and putamina.
B, Axial T1-weighted MR image shows low T1 signal intensity.
C, Axial gadolinium-enhanced T1-weighted MR image shows mild patchy enhancement of basal ganglia. No enhancement is present in thalami.
D, Single-voxel MR spectroscopic recording (TE, 144 ms) shows lactate peak (*arrow*). Patient did not have reduced diffusion in region of lesions (not shown).
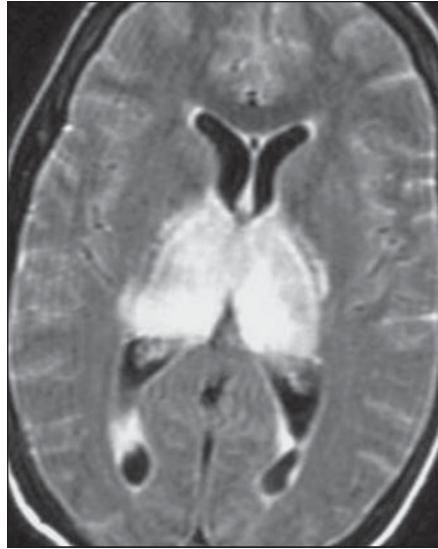
Fig. 8—48-year-old woman with West Nile encephalitis. Axial T2-weighted MR image shows hyperintensity and expansion of both thalami. Increased signal intensity is present within sulci.
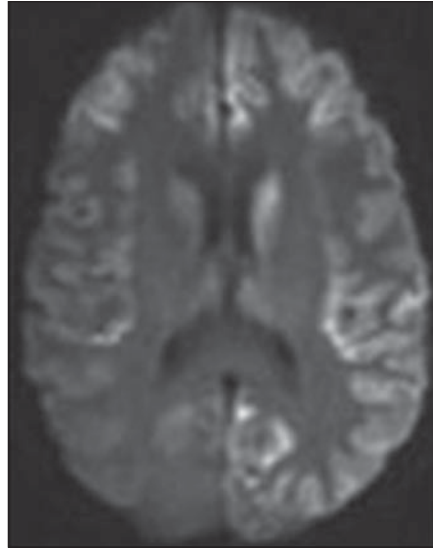
Fig. 9—70-year-old man with sporadic Creutzfeldt-Jakob disease. Axial diffusion-weighted MR image shows bilateral high signal intensity in caudate nuclei and thalami. Prominent cortical ribboning is present.
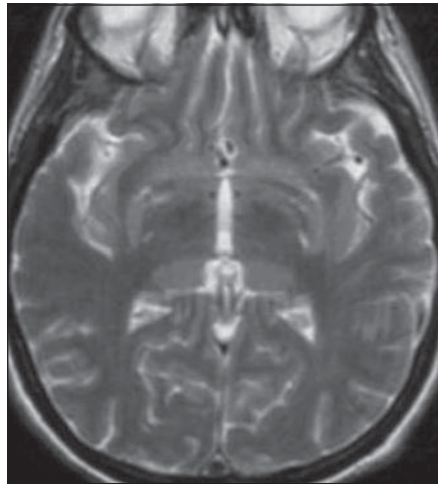
A
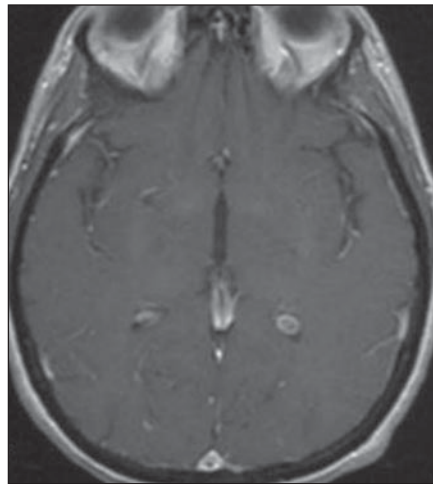
B

Fig. 10—23-year-old woman with variant Creutzfeldt-Jakob disease.
A, Axial T2-weighted MR image shows T2 hyperintensity in both pulvinars (pulvinar sign).
B, Gadolinium-enhanced T1-weighted MR image shows no associated enhancement.

A

B
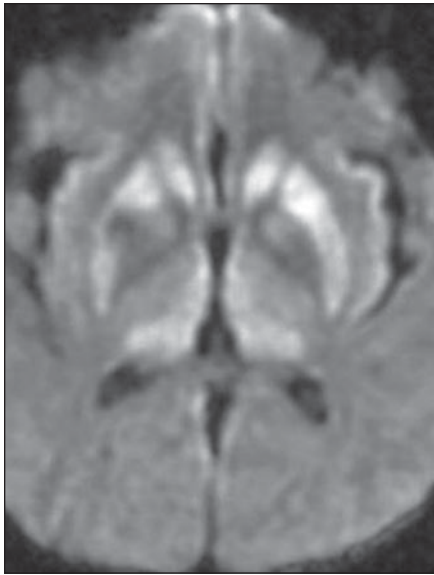
Fig. 11—26-year-old woman with variant Creutzfeldt-Jakob disease. Axial diffusion-weighted MR image shows reduced diffusion involving pulvinar and dorsomedial thalami (hockey stick sign). High signal intensity also is present in both basal ganglia. No cortical ribboning is present.
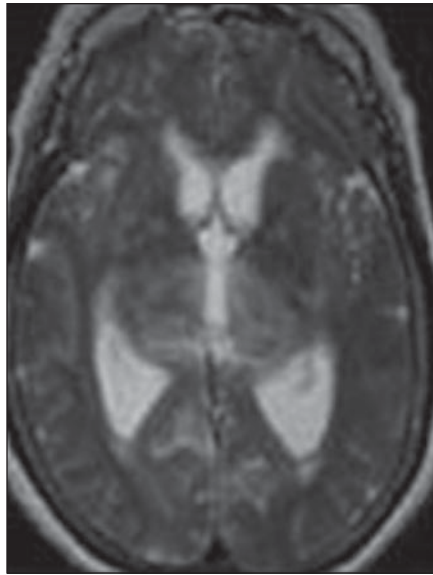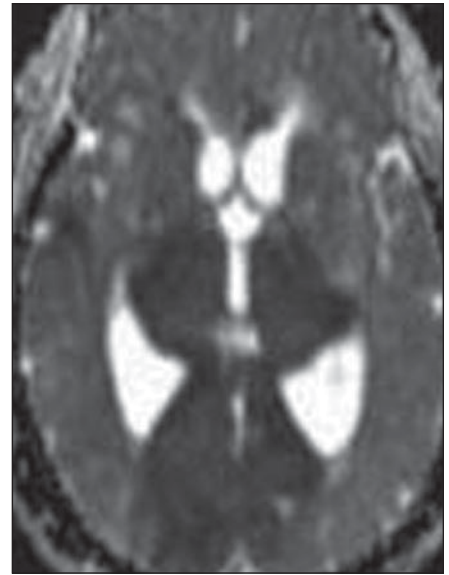
Fig. 12—60-year-old man with top of basilar syndrome.
A, Axial T2-weighted MR image shows bilateral increased signal intensity in thalami and medial occipital lobes.
B, Axial apparent diffusion coefficient map shows low signal intensity consistent with reduced diffusion and cytotoxic edema.
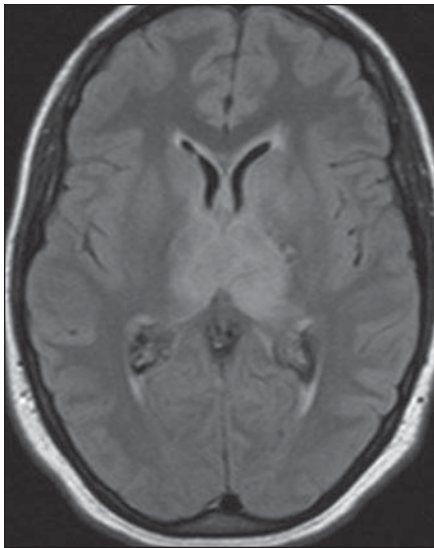
A
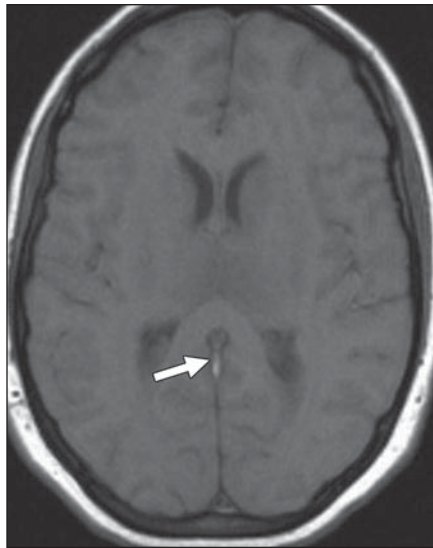
B
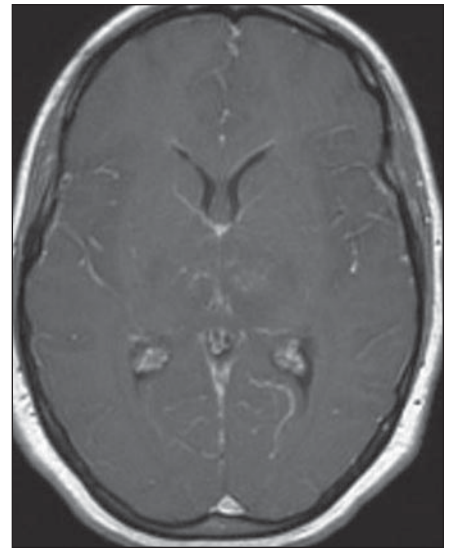
C

Fig. 13—47-year-old woman with sinus deep venous thrombosis.
A, Axial T2-weighted FLAIR MR image shows increased signal intensity in both thalami.
B, Axial T1-weighted MR image shows low signal intensity in both thalami. Focus of high signal intensity (*arrow*) in straight sinus is consistent with clot.
C, Axial T1-weighted gadolinium-enhanced MR image shows patchy enhancement in both thalami.

(Fig. 13 continues on next page)

D

E

F
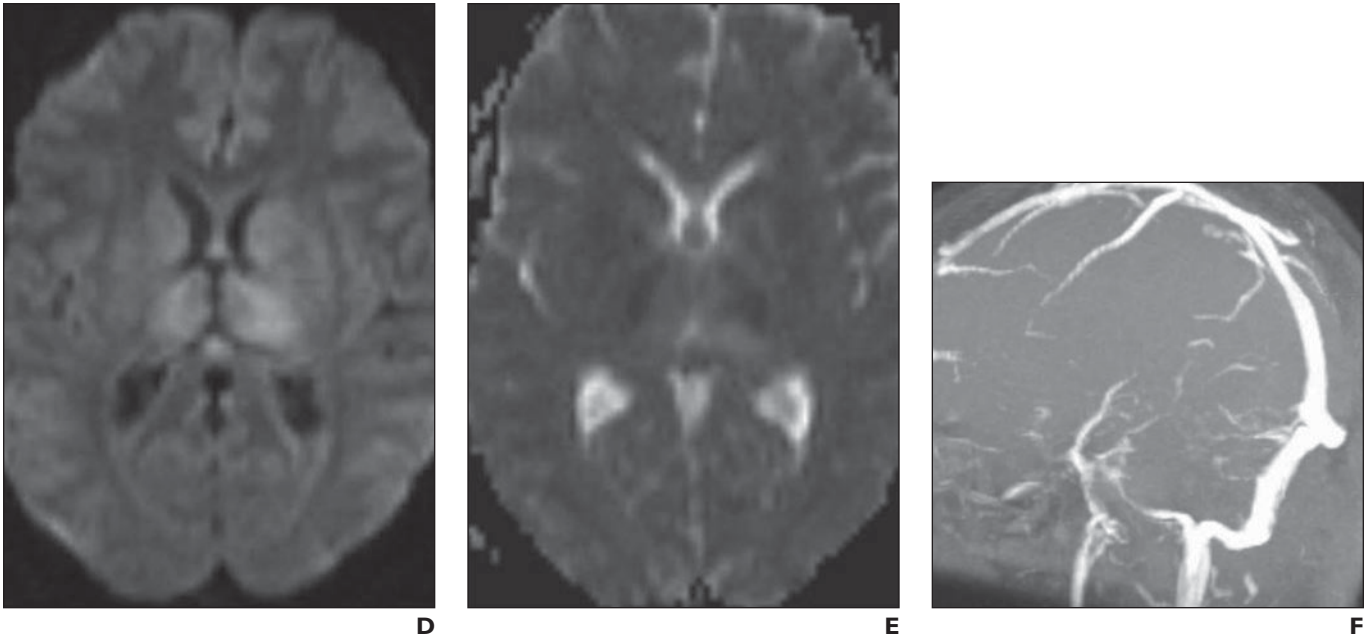
Fig. 13 (continued)—47-year-old woman with sinus deep venous thrombosis.
D, Axial diffusion-weighted image shows heterogeneously high signal intensity in both thalami.
E, Apparent diffusion coefficient map shows low signal intensity consistent with cytotoxic edema.
F, MR venogram shows loss of flow-related signal intensity in straight sinus and right transverse sinus, consistent with thrombosis.

A

B

C
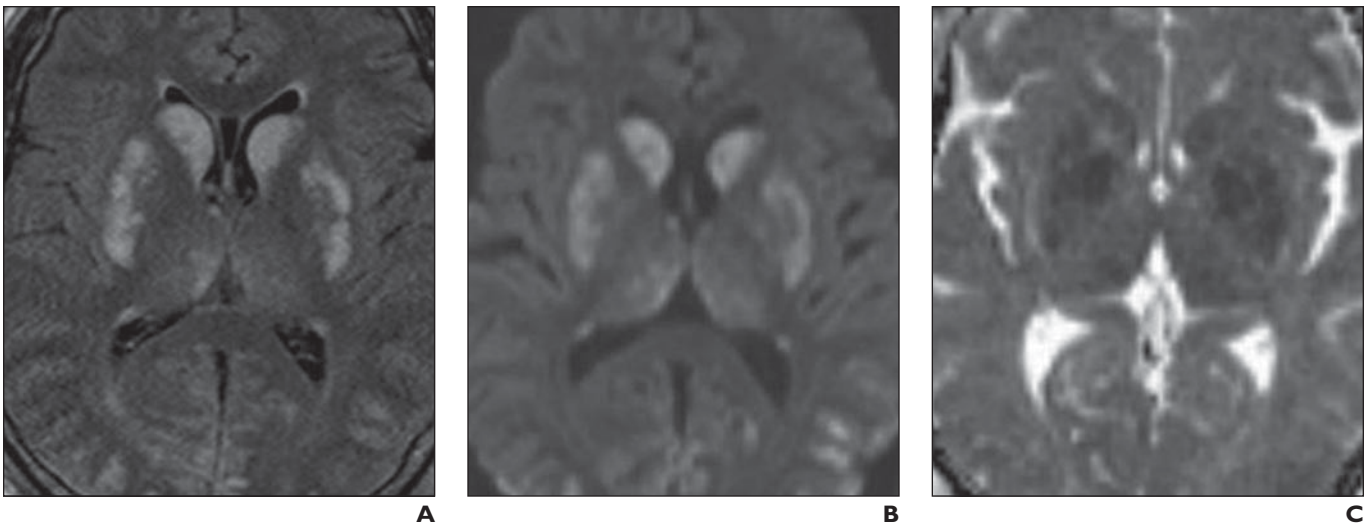
Fig. 14—64-year-old man with prolonged hypoxic event.
A, Axial T2-weighted FLAIR MR image shows hyperintensity in both basal ganglia and thalami.
B, Axial diffusion-weighted MR image shows high signal intensity.
C, Apparent diffusion coefficient map shows low signal intensity consistent with cytotoxic edema.
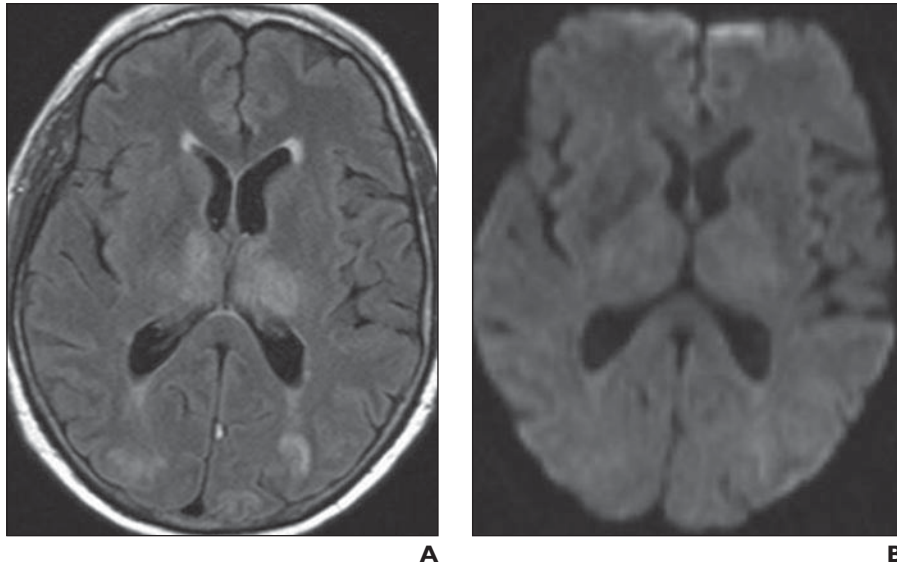
Fig. 15—32-year-old man with posterior reversible encephalopathy syndrome.
A, Axial FLAIR MR image shows symmetric T2 hyperintensity in posterior white matter and both thalami.
B, Axial diffusion-weighted MR image shows no reduced diffusion.

FOR YOUR INFORMATION

This article is available for CME credit. See www.arrs.org for more information.